Analysis of Sensorless Model Control DC-DC Converter in CCM

Yudai Furukawa*, Shingo Watanabe*, Hidenori Maruta*, Nobumasa Matsui**, Ilhami Colak*** and Fujio Kurokawa*
* Graduate School of Engineering, Nagasaki University, Nagasaki, Japan
** Faculty of Engineering, Nagasaki Institute of Applied Science, Nagasaki, Japan
*** Faculty of Engineering and Architecture, Gelisim University, Istanbul, Turkey

Abstract**-- We have proposed the sensorless model control based on the static model equation of the dc-dc converter that is able to change the bias value corresponding to changes of the load current, the input voltage and output voltage. The sensorless model control can regulate the output voltage. On the other hand, the transient response of output voltage is not improved. Therefore, an improvement of the transient response is carried out by adding the transient improvement function which changes a bias value drastically for a short time at the start of the transient state. The purpose of this paper is to indicate the parameter setting of the transient improvement function that improves the transient response by the simulation analysis under changing the circuit condition.**

Index Terms**--dc-dc converter, digital control, sensorless model control, transient improvement function**

I. INTRODUCTION

In recent years, a lot of information caused by the diffusion of the ICT equipment is communicated via the data center [1]. It is expected that the amount of the information is going to increase. Therefore, the high efficient usage of energy is required in the data center [2]. The digital control which has the energy management function is attracting attention to use energy in the high efficiency [3]-[6]. The number of power supply unit in operation is decided by the energy management because energy flow in the data center is controlled corresponding to the condition of the system. When the load requires the much energy, the power supply unit has to return quickly from standby mode to the operation [7]. In such condition, the operating point of the power supply must be controlled rapidly by increasing the on time of the main switch.

We have proposed the model control based on the static model equation of the dc-dc converter that is able to change the bias value corresponding to changes of the load current, the input voltage and output voltage. The model control can realize the quick change of the operating point and the satisfactory regulation characteristics. The model control can realize the quick change of the operating point and the satisfactory regulation characteristics. The detection resistor is necessary to detect the output current and it causes increases of the number of component and loss of power. As a solution of this problem, a sensorless model control that predicts the output current has been proposed [8]-[10]. The sensorless model control can realize the satisfactory regulation characteristics as well as the model control which detects the output voltage. However, the improvement of the transient response is not obtained. An improvement of the transient response is carried out by adding the transient improvement function which changes a bias value drastically for a short time at the start of the transient state. The transient improvement function can suppress the first overshoot or undershoot in the transient state and improve the transient response.

This paper presents the parameter setting of the transient improvement function that improves the transient response by the simulation analysis under changing the circuit condition.

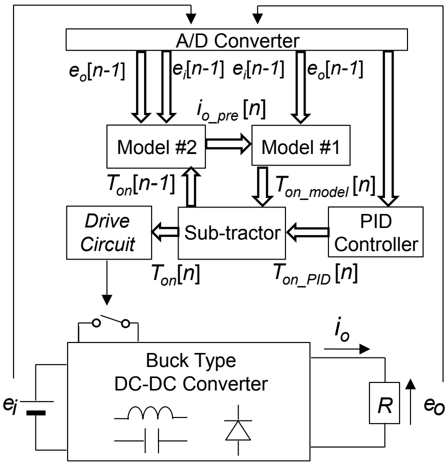

Fig. 1. Digital control dc-dc converter and digital control circuit.

II. OPERATION PRINCIPLE

Figure 1 shows the digital control dc-dc converter and the digital control circuit. A main circuit is a buck type dc-dc converter. In this figure, e_i is the input voltage, e_o is the output voltage, R is the load resistor and i_o is the output current. e_i and e_o are detected and inputted to the digital control circuit. Then the on-time is determined by the digital control circuit. The output current was detected in the existing model control. Therefore, the sensing resistor was needed. In the propose method, it is eliminated because i_o is predicted in Model #2. In the digital control circuit, e_i and e_o are inputted into the pre-amplifier. They are amplified by A_{ei} and A_{eo}, respectively. A_{ei} and A_{eo} are the gain of each pre-amplifier. The digital controller consists of the output current predictor (Model #1), the static model controller (Model #2) and the PID controller. $e_i[n\text{-}1]$ is sent to

Authorized licensed use limited to: Istanbul Gelisim Univ. Downloaded on February 14,2025 at 07:14:56 UTC from IEEE Xplore. Restrictions apply.

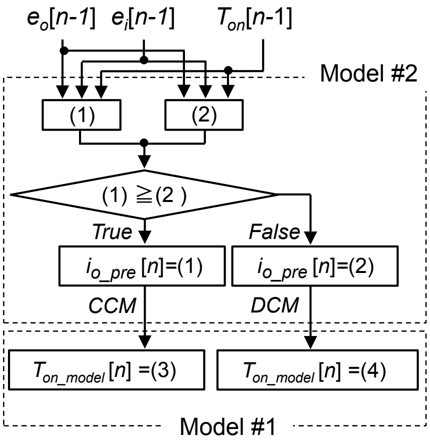

Fig. 2. Flowchart of sensorless model control.

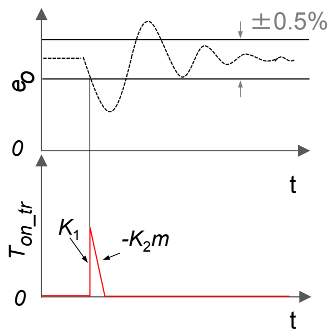

Fig. 3. Principle of transient improvement function.

Model #1 and Model #2 and also $e_o[n\text{-}1]$ is sent to Model#1 and PID controller.

A. Model Control

In Model #1, the predicted output current $i_{o\_pre}[n]$ is calculated by using the digital value $T_{on}[n\text{-}1]$ of on-time, $e_i[n\text{-}1]$ and $e_o[n\text{-}1]$. The equation for the prediction of output current is shown below:

$$i_{o\_pre\_CCM}[n] = \frac{T_{on}[n](\frac{e_i[n-1]}{a}+V_D) - N_{Ts}(\frac{e_o[n-1]}{b}+V_D)}{rN_{Ts}} \tag{1}$$

$$i_{o\_pre\_DCM}[n] = \frac{(\frac{e_i[n-1]}{a}-\frac{e_o[n-1]}{b})(\frac{e_i[n-1]}{a}+V_D)T_s T_{on}^2[n-1]}{2L(\frac{e_o[n-1]}{b}+V_D)} \tag{2}$$

In the transient state, the predicted current becomes oscillatory due to the fluctuation of the on-time. Therefore, the damping ratio is used to suppress the oscillation of the predicted current. Although it can bring the stable operation of the sensorless model control, the predicted output current cannot trace the output current quickly. The bias value $T_{on\_m}[n]$ is calculated in Model #2 by using $i_{o\_pre}[n]$ and $e_i[n]$. There are two equations for the calculation of $T_{on\_m}[n]$. They are expressed as follows:

$$T_{on\_m\_CCM}[n] = \frac{N_{Ts}}{(\frac{e_i[n]}{a}+V_D)}\left(E_o^* + r i_{o\_pre}[n] + V_D\right) \tag{3}$$

$$T_{on\_m\_DCM}[n] = N_{Ts}\sqrt{\frac{2L i_{o\_pre}[n](E_o^*+V_D)}{(\frac{e_i[n]}{a}+V_D)(\frac{e_i[n]}{a}-E_o^*)T_s}} \tag{4}$$

In these equations, E_o^* is the target value of the output voltage. T_s is the switching period and N_{Ts} are the resolution of digital PWM generator. r and V_D are internal loss and diode forward voltage. r is omitted in (2) because it does not almost affect on the calculation result of (4). Also, a and b are given by

$$a = A_{ei} G_{AD\_ei} \tag{5}$$

$$b = A_{eo} G_{AD\_eo} \tag{6}$$

where G_{AD_ei} and G_{AD_eo} are the gains of the A-D converter for e_i and e_o. The index n denotes the sampling point obtained at the n-th switching period. Figure 2 shows the flowchart of the sensorless model control. Equations (1) and (2) are switched and applied depending on the operation modes of the dc-dc converter, which are the current continuous mode (CCM) and the current discontinuous mode (DCM). Equations (1) and (2) are calculated simultaneously and compared with each other. Larger values of them are applied as $i_{o\_pre}[n]$ and the operation mode of the dc-dc converter is judged. $T_{on\_m}[n]$ is calculated according to the operation mode. The model control can adjust the operating point correctly according to i_o, and therefore can regulate e_o.

B. Transient Improvement Function

The transient improvement function $T_{on\_tr}[m]$ that changes the bias value rapidly is applied to realize the quick response. It is represented by

$$T_{on\_tr}[m] = k_1 - k_2 m T_s \tag{7}$$

Coefficient k_1 is the peak value of $T_{on\_tr}[m]$, k_2 is the coefficient of decrement and m is the number of the switching (or control) period after the start of addition of $T_{on\_tr}[m]$. Figure 3 shows the principle of the transient improvement function. When the output voltage exceeds the threshold value, this function is applied and the bias value is changed. $T_{on\_tr}[m]$ increase to k_1 immediately, and then it decreases depending on k_2. When $T_{on\_tr}[m]$ becomes zero or less, the adjunction is end. The improvement of the transient characteristics of the output voltage is obtained. The final on-time $T_{on}[n]$ is shown as follows:

$$T_{on}[n] = T_{on\_PID}[n] + T_{on\_m}[n] + T_{on\_tr}[m] \tag{8}$$

In (8), $T_{on\_PID}[n]$, $T_{on\_m}[n]$ and $T_{on\_tr}[m]$ are the

Authorized licensed use limited to: Istanbul Gelism Univ. Downloaded on February 14,2025 at 07:14:56 UTC from IEEE Xplore. Restrictions apply.

calculation results of the PID controller, the model controller and the transient improvement function, respectively.

III. Simulation Result

In this section, the effectiveness of the transient improvement function is verified when the circuit condition is changed. The setting of parameters of the transient improvement function is considered by the simulation analysis. The switching frequency f_s is 100 kHz. Parameters of the circuit are as follows: e_i = 20 V, the reference voltage of output voltage E_O* = 5 V, L = 196 μH and C = 891 μF. The resolution of A-D converter is 11 bits and N_{Ts} is 2000. The evaluation items are the undershoot, overshoot and convergence time of the output voltage. Figure 4 shows the transient characteristics of e_O when parameters of the transient improvement function is changed. In this case, the load varies stepwise from 0.5 A to 1 A. The tendency of the transient characteristics shows that each item is improved when k_2 is set to a large value. Figure 5 shows the transient response of e_O in existing sensorless model control and k_1 = 210, 850, 1060. In figure 5 (b), the satisfactory characteristics are obtained compared to existing sensorless model control because the transient improvement function is valid for a short time and the first undershoot is suppressed well. In Fig. 5 (c), an overcompensation which adversely affects on an overshoot of e_O is occurred since the transient improvement function becomes enable for about four switching period. Similarly, an overcompensation is occurred in Fig. 5 (c). In Fig. 5 (d), the undershoot of e_O is not suppressed enough because the added bias by k_1 is small. Next, Figure 6 shows the transient response of e_O in each capacitance. The undershoot of e_O is suppressed and the waveform of e_O becomes gradually in setting C to a large value. Figure 7 shows the transient characteristics of e_O when C is 10mF. A satisfactory response is obtained in this case by addition of the transient improvement function for only one switching period. Even when k_1 is set to a small value, a satisfactory response is also obtained by addition of the transient improvement function for several switching periods.

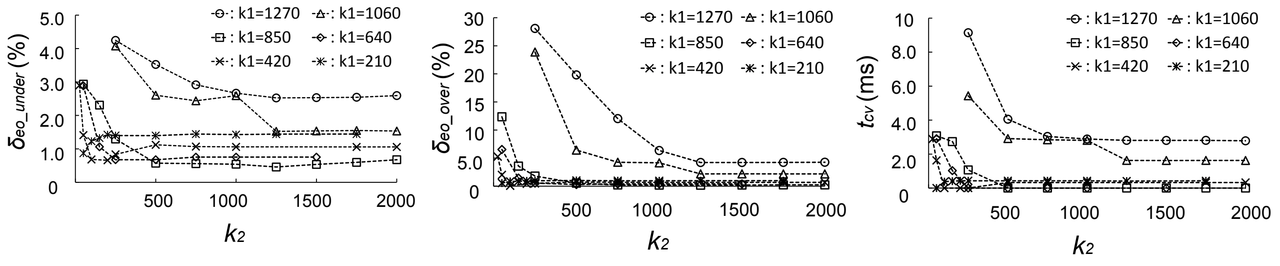

(a) (b) (c)

Fig. 4. Transient characteristics of output voltage, e_O, when parameters of transient improvement function are changed: (a) undershoot, δ_{eo_under}, (b) overshoot, δ_{eo_over}, and (c) convergence time, t_{cv}.

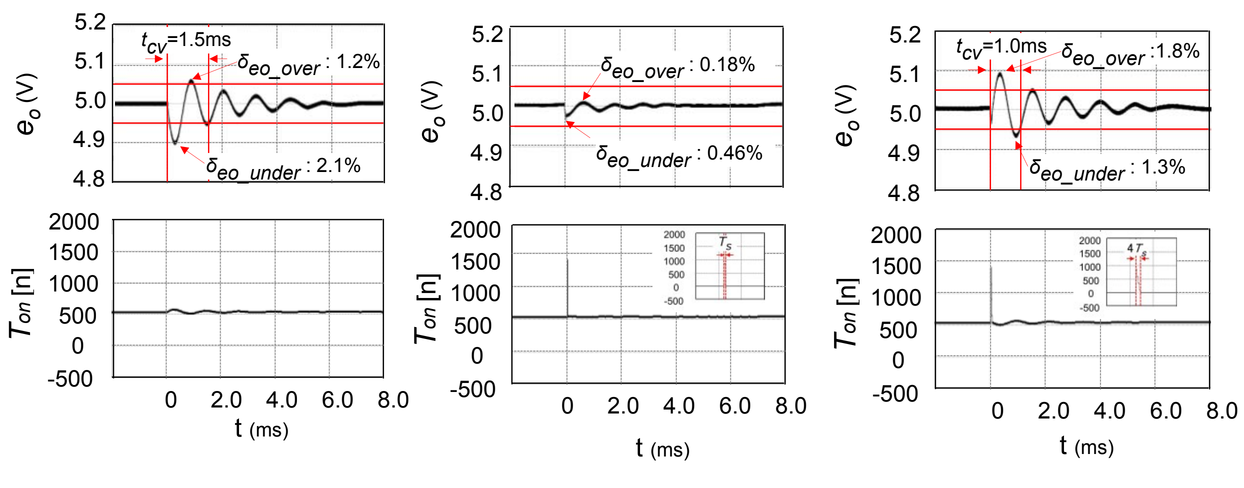

(a) (b) (c)

Fig. 5. Waveforms of output voltage, e_O, (top) and transient improvement function, $T_{on\_tr}[n]$, (bottom) in transient state: (a) existing sensorless model control, (b) k_1 = 850 and k_2 = 1250 in proposed method, (c) k_1 = 850 and k_2 = 250 in proposed method, (d) k_1 = 1060 and k_2 = 1250 in proposed method, and (e) k_1 = 210 and k_2 = 1250 in proposed method (continue).

Authorized licensed use limited to: Istanbul Gelism Univ. Downloaded on February 14,2025 at 07:14:56 UTC from IEEE Xplore. Restrictions apply.

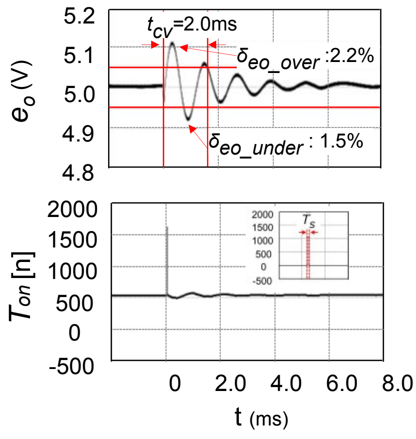

(d)

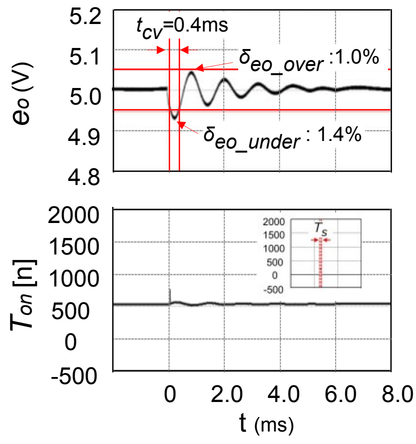

(e)

Fig. 5. Waveforms of output voltage, e_O, (top) and transient improvement function, $T_{on\_tr}[n]$, (bottom) in transient state: (a) existing sensorless model control, (b) k_1 = 850 and k_2 = 1250 in proposed method, (c) k_1 = 850 and k_2 = 250 in proposed method, (d) k_1 = 1060 and k_2 = 1250 in proposed method, and (e) k_1 = 210 and k_2 = 1250 in proposed method (continued).

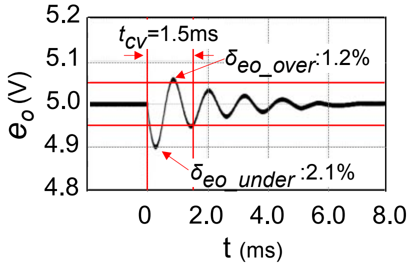

(a)

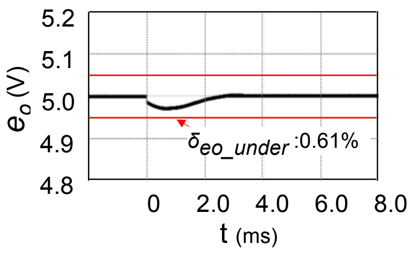

(b)

Fig. 6. Waveforms of output voltage, e_O, in transient state when output capacitor, C, is changed: (a) C = 891 μF, and (b) C = 10 mF.

When k_1 is set to too large value or k_2 is set to too small value, the transient response becomes worse because of an overcompensation. The transient response of e_O is shown in fig.7 in the case of C = 10mF. In Fig. 8 (b), the transient improvement function suppresses the undershoot of e_O compared to Fig. 8(a). Next, Fig. 9 shows the transient characteristics of e_O in the case of load step from 0.5A to 1A and 4A. The undershoot and overshoot of e_O become large by the wide load step. Figure 10 also shows transient characteristics in the case of the load step from 0.5A to 4A. k_1 should be set a large value enough to suppress the overshoot or undershoot of e_O since the undershoot or overshoot of e_O becomes large by a wide load step. Even when the load changes from 0.5 A to 4 A, k_1 is set to a proper value enough to suppress the undershoot of e_O. Figure 11 shows the transient response of e_O in the case of the load step from 0.5A to 4A. In this case, the undershoot and overshoot of e_O are large compared to the load step from 0.5A to 1A. Therefore, the undershoot cannot be suppressed in setting k_1 to 850. In Fig. 11(b), a superior transient response is obtained because the undershoot is adequately suppressed. The transient response is improved drastically when the k_1 and k_2 are set to large value and one switching period. In contrast, a large overshoot occurs because there is an overcompensation by large k_1 in Fig. 11(c).

From the results, the transient response is able to be improved by the transient improvement function added to suppress the first undershoot at the start of the transient state. In any case, although the first undershoot of e_O is suppressed by the addition of the transient improvement function for one switching period at the start of the transient state, a value of k_1 should be set proper one corresponding to an amount of the undershoot of e_O.It leads to an improvement of the transient response of e_O

IV. Conclusion

In this paper, the effectiveness of the transient improvement function is confirmed and the setting of parameters of the transient improvement function is considered by the simulation analysis. From the results, the transient response can be improved by the transient improvement function added to suppress the first undershoot at the start of the transient state. In any case, although the first undershoot of output voltage is

Authorized licensed use limited to: Istanbul Gelism Univ. Downloaded on February 14,2025 at 07:14:56 UTC from IEEE Xplore. Restrictions apply.

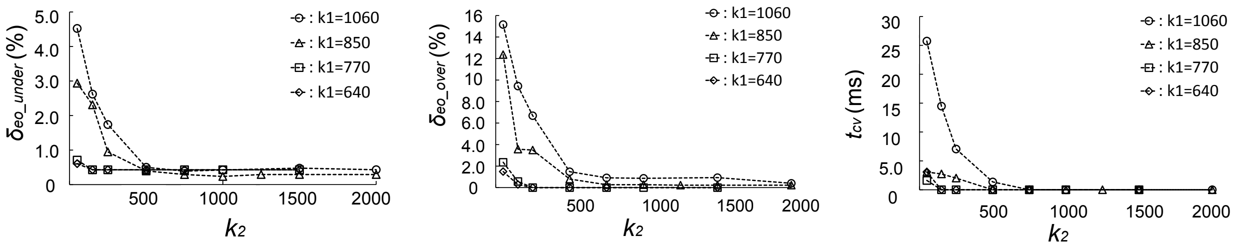

(a) (b) (c)

Fig. 7. Transient characteristics of output voltage, e_o, when parameters of transient improvement function are changed and output capacitor, C, is set to 10 mF: (a) undershoot, δ_{eo_under}, (b) overshoot, δ_{eo_over}, and (c) convergence time, t_{cv}.

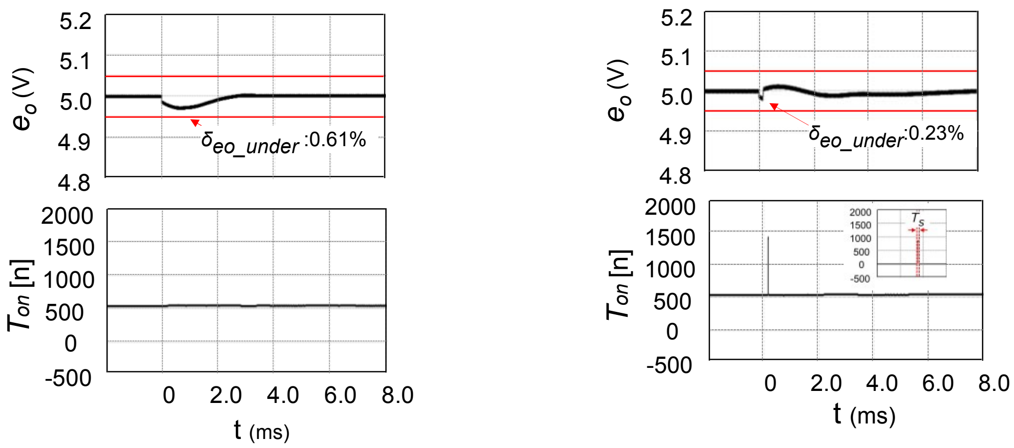

(a) (b)

Fig. 8. Waveforms of output voltage, e_o, (top) and transient improvement function, $T_{on\_tr}[n]$, (bottom) in transient state: (a) existing sensorless model control, and (b) k_1 = 850 and k_2 = 1250 in proposed method.

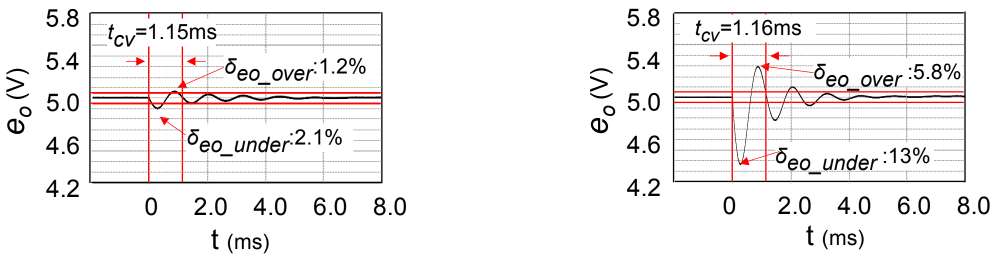

(a) (b)

Fig. 9. Waveforms of output voltage, e_o, in transient state in case of: (a) from 0.5 A to 1 A, and (b) from 0.5 A to 4 A.

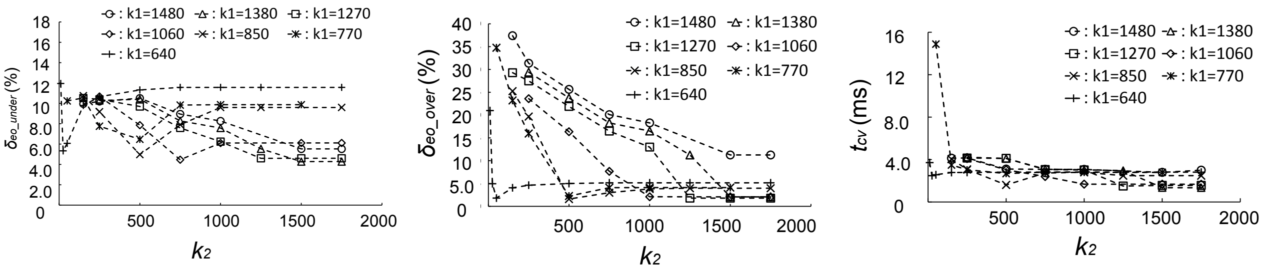

(a) (b) (c)

Fig. 10. Transient characteristics of output voltage, e_o, when parameters of transient improvement function are changed and load step is from 0.5A to 4A: (a) undershoot, δ_{eo_under}, (b) overshoot, δ_{eo_over}, and (c) convergence time, t_{cv}.

Authorized licensed use limited to: Istanbul Gelism Univ. Downloaded on February 14,2025 at 07:14:56 UTC from IEEE Xplore. Restrictions apply.

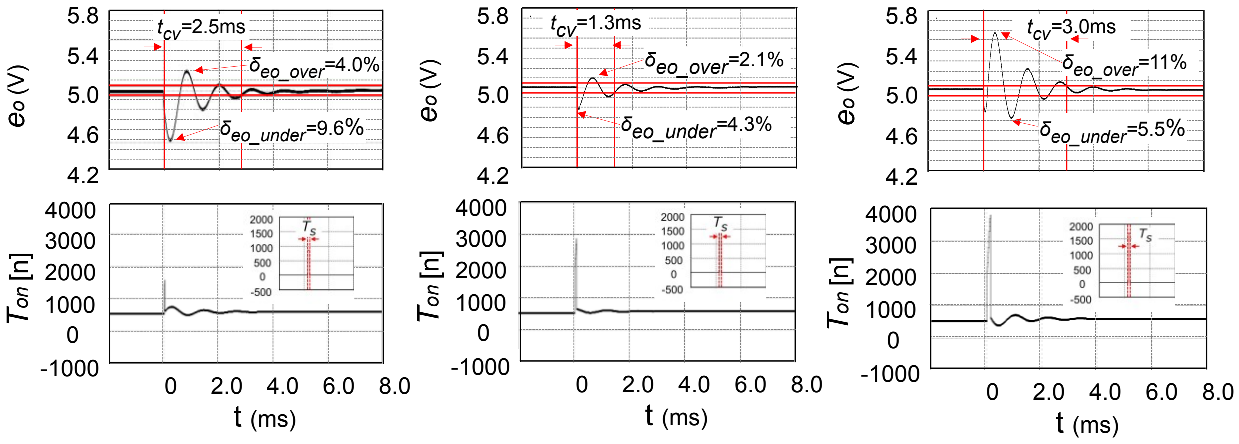

(a) (b) (c)

Fig. 11. Waveforms of output voltage, e_o, (top) and transient improvement function, $T_{on\_tr}[n]$, (bottom) in transient state: (a) k_1 = 850 and k_2 = 1750 in proposed method, (b) k_1 = 1380 and k_2 = 1750 in proposed method, and (c) k_1 = 1480 and k_2 = 1750 in proposed method.

suppressed by adding the transient improvement function for one switching period at the start of the transient state, a value of k_1 should be set appropriate one to deal with an amount of the undershoot of output voltage.

REFERENCES

[1] M. Martino, G. Mutani and R. Miceli, "Smart Energy Users: ICT Instruments for the Consumer Awareness" Proc. of International Telecommunications Energy Conference, pp. 835-840, Oct. 2015.

[2] H. Yajima, T. Babasaki, Y. Ooi, K. Hirose, "Energy-saving and Efficient use of Renewable Energy by introducing an 380 VDC Power-supply System in Data Centers" Proc. of International Telecommunications Energy Conference, pp. 946-949, Oct. 2015.

[3] L. Corradini, E. Orietti, P. Mattavelli and S. Saggini, "Digital hysteretic voltage-mode control for dc-dc converters based on asynchronous sampling," *IEEE Trans. Power Electronics*, Vol. 24, No. 1, pp. 201-211, Jan. 2009.

[4] G. Feng, E. Meyer and Y. Liu, "A new digital control algorithm to achieve optimal dynamic performance in dc-to-dc converters," *IEEE Trans. on Power Electronics*, pp. 1489-1498, Jul. 2007.

[5] R. C. N. Pilawa-Podgurski, W. Li, I. Celanovic and D. J. Perreault, "Integrated cmos dc-dc converter with digital maximum power point tracking for a portable thermophotovoltaic power generator," Proc. of IEEE Energy Conversion Congress and Exposition, pp. 197-204, Sep. 2011.

[6] K. De Cuyper, M. Osee, F. Robert and P. Mathys, "A digital plat form for real-time simulation of power converters with high switching," in Proc. IEEE Power Electronics and applications, pp. 1-10, Sep. 2011.

[7] T. Ueno, T. Miyazaki, T, Ogawa and T. Itakura, "A 600 mA, constant on-time controlled DC-DC converter with 67% conversion efficiency at an output current of 23 μA," in Proc. IEEE Applied Power Electronics Conference and Exposition, pp.1932-1935, Mar. 2014.

[8] F. Kurokawa and S.Hirotaki, "Model control dc-dc converter without current detection," in Proc. IEEE International Conference on Intelligent Green Building and Smart Grid, pp. 1-5, Apr. 2014.

[9] F. Kurokawa and S. Hirotaki, "A novel sensorless model control dc-dc converter," in Proc. IEEE Renewable Energy Research and Application , pp 663 - 667, Oct. 2014.

[10] F. Kurokawa and S.Hirotaki, "A new high performance dc-dc converter with sensoress model reference modification" Proc. of International Telecommunications Energy Conference, pp. 1-5, Oct. sep. 2014.

Authorized licensed use limited to: Istanbul Gelism Univ. Downloaded on February 14,2025 at 07:14:56 UTC from IEEE Xplore. Restrictions apply.